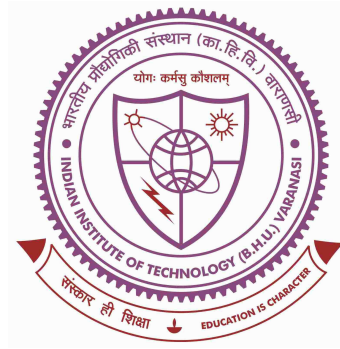

Design and Development of Multi-Output Multi-level Converter for Multi-Motor Drives



*A thesis submitted in partial fulfillment of the requirements
for the award degree
Doctor of Philosophy*

by

Dhawal Dwivedi

DEPARTMENT OF ELECTRICAL ENGINEERING

Indian Institute of Technology

(Banaras Hindu University), Varanasi

Varanasi-221005

INDIA

Roll No: 21081005

October 2025

Certificate

It is certified that the work contained in this thesis entitled “**Design and Development of Multi-Output Multi-level Converter for Multi-Motor Drives**” by **Dhawal Dwivedi** has been carried out under my supervision and that it has not been submitted elsewhere for a degree.

It is further certified that the student has fulfilled all the requirements of the Comprehensive Examination, Candidacy, and SOTA for the award of Ph.D. Degree.



Supervisor

Dr. Chinmaya K A

Assistant Professor

Dept. of Electrical Engg.

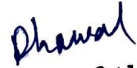
IIT(BHU), Varanasi

Uttar Pradesh, INDIA.

Declaration

I, Dhawal Dwivedi, certify that the work embodied in this thesis titled “**Design and Development of Multi-Output Multi-level Converter for Multi-Motor Drives**” is my own bonafide work and has been carried out by me under the supervision of **Dr. Chinmaya K A** from July-2021 to July-2025, at the Department of Electrical Engineering, Indian Institute of Technology (Banaras Hindu University), Varanasi (UP).

To the best of my knowledge, it is an original work, both in terms of research content and narrative, and has not been submitted elsewhere, in part or in full, for a degree. Further, due credit has been attributed to the relevant state-of-the-art and collaborations with appropriate citations and acknowledgments, in line with established norms and practices.


Signature of the student

(Dhawal Dwivedi)

Roll No. 21081005

Dept. of Electrical Engg.

IIT(BHU), Varanasi

Uttar Pradesh, INDIA.

Date: 09/10/25

Place: Varanasi

Certificate by the supervisor

It is certified that the above statement made by the student is correct to the best of our knowledge.



Dr. Chinmaya K A

(Supervisor)


Signature of Head of Department

Prof. R. K. Singh

आचार्य एवं विभागाध्यक्ष / PROFESSOR & HEAD
विद्युतीय अभियांत्रिकी विभाग / Department of Electrical Engineering
भारतीय प्रौद्योगिकी संस्थान / Indian Institute of Technology
(काशी हिन्दू विश्वविद्यालय) / (Banaras Hindu University)
Varanasi, U.P. (INDIA)

Copyright Transfer Certificate

Title of the Thesis: "Design and Development of Multi-output Multi-level Converter for Multi-Motor Drives".

Name of Student: Dhawal Dwivedi

Copyright Transfer

The undersigned hereby assigns to the Indian Institute of Technology (Banaras Hindu University), Varanasi all rights under copyright that may exist in and for the above thesis submitted for the award of the Doctor of Philosophy.

Date: 09/10/25

Place: Varanasi

Dhawal

(Dhawal Dwivedi)

Note: However, the author may reproduce or authorize others to reproduce material extracted verbatim from the thesis or derivative of the thesis for author's personal use provided that the source and the Institute's copyright notice are indicated.

Dedicated to family.

List of Figures

1.1	Dual motor drive system. (a) Individual motor drive system. (b) MIDP motor drive system.	2
2.1	Three-phase back to back converter.	8
2.2	Application of the B2B converter in grid-tied wind turbine systems.	8
2.3	B4 converter.	9
2.4	Four-leg converter.	9
2.5	Five-leg converter.	10
2.6	Nine-switch inverter.	11
2.7	Z-source modified NSI.	12
2.8	Six-switch dual-output inverter.	12
2.9	Three-switch dual-output inverter.	13
2.10	Three-phase three-port MLI (TPTPMLI).	14
2.11	Three-level twin drive inverter (TL-TDI).	16
2.12	Neutral point piloted (NPP).	17
2.13	Three phase schematics of dual-output flying capacitor inverter (DO-FCI).	18
2.14	Three phase schematics of reduced switch count dual-output T-type (RSC-DT) converter.	20
2.15	Three phase schematics of dual-output neutral-point-clamped three-level inverter (DO-NPC-TLI).	23
2.16	Three phase schematics of neutral-point clamped dual-output (NPC-DO) converter.	26
2.17	Generalized multi-input multi-output circuit diagram of (a) the CMOM converter and (b) the M-CMOM converters.	27
2.18	Circuit diagram of the M-CMOM converter ($m = 2$ and $n = 5$).	28
2.19	The evaluation process of the maximum allowable phase shift for the NPP Converter at modulation indices $m_1 = m_2 = 0.8$ reveals that: (a–c) when the phase shift varies from 0° to 30° , both reference signals remain within the permissible operating boundaries; (d) however, beyond 30° , the reference vectors exceed the feasible region, violating the converter’s modulation constraints.	35
3.1	Proposed three-level dual-output ANPC converter.	38
3.2	Operating states of the proposed TLDO-ANPC. (a) $v_{x1} = 0$ and $v_{x2} = -V_{dc}/2$. (b) $v_{x1} = V_{dc}/2$ and $v_{x2} = 0$. (c) $v_{x1} = V_{dc}/2$ and $v_{x2} = -V_{dc}/2$	41

3.3	DC-link capacitor voltage ripple in few-cycle for C_1 and C_2 of the TLDO-ANPC converter through proposed PWM under CF mode with $m_1 = m_2 = 1$, $f_1 = f_2 = 50$ Hz.	45
3.4	Normalized DC-link capacitor voltage ripple for C_1 of the TLDO-ANPC converter under CF mode with $m_1 = 1$ and $\theta_{L1} = 7.16^\circ$	46
3.5	Graphical depiction of the region of operation and switching states.	47
3.6	Projections of reference signals onto the TLDO-ANPC converter's boundary region under (a) CF with $m_1 = 1$, $m_2 = 0.9$, (b) CF with $m_1 = m_2 = 0.9$ and phase shift of 30° , (c) DF with $m_1 = m_2 = 1$	49
3.7	IPD PWM scheme for TLDO-ANPC in the (a) CF mode with $m_1 = 1$, $m_2 = 0.9$ and $\phi = 0^\circ$, (b) CF mode with $m_1 = m_2 = 0.9$ and $\phi = 30^\circ$, (c) DF mode with $m_1 = m_2 = 1$, $f_1 = 50$ and $f_2 = 100$ Hz.	50
3.8	Hardware setup the proposed converter consisting of (I) Digital signal oscilloscope. (II) DSP TMS320F28335. (III) TLDOV-ANPC converter with its gate driver. (IV) Resistive loads. (V) Inductive loads. (VI) Voltage and current probe (VII) DC power supply.	52
3.9	Experimental result in CF mode (a) output voltages (v_{A1}, v_{A2}) and currents (i_{A1}, i_{A2}) with $m_1 = m_2 = 1$, (b) DC-link capacitor voltage balancing with $m_1 = m_2 = 1$, (c) output voltages (v_{A1}, v_{A2}) and currents (i_{A1}, i_{A2}) with $m_1 = 1$, $m_2 = 0.9$	53
3.10	Simulation results for output voltages (v_{A1}, v_{A2}) and currents (i_{A1}, i_{A2}) (a) CF mode with $m_1 = m_2 = 1$, when both load currents are flowing from the output terminal to the DC-link capacitor, (b) CF mode with $m_1 = m_2 = 1$, when i_{A1} is flowing from the output terminal to the DC-link capacitor, and i_{A2} is flowing from DC-link to the load, (c) DF mode with $m_1 = m_2 = 1$ and $f_1 = 50$ Hz, $f_2 = 100$ Hz when both load current are flowing from the output terminal to the DC-link capacitor.	54
3.11	(a) Experimental result for output voltages (v_{A1}, v_{A2}) and currents (i_{A1}, i_{A2}) in CF mode, $m_1 = m_2 = 0.9$ and $\phi = 30^\circ$. (b) Experimental result of DC-link capacitor voltage for three-phase in CF mode with $m_1 = 1$, $m_2 = 1$	55
3.12	Experimental result (a) output voltages (v_{A1}, v_{A2}) and currents (i_{A1}, i_{A2}) in CF mode, $m_1 = 0.8$, $m_2 = 0.7$ and $\phi = 30^\circ$, (b) output voltages (v_{A1}, v_{A2}) and currents (i_{A1}, i_{A2}) in CF mode, $m_1 = m_2 = 0.9$ and $\phi = 60^\circ$, (c) output voltages (v_{A1}, v_{A2}) and currents (i_{A1}, i_{A2}) in DF mode, $m_1 = m_2 = 1$ and $f_1 = 50$ Hz, $f_2 = 60$ Hz.	56
3.13	Experimental result for (a) output voltages (v_{A1}, v_{A2}) and currents (i_{A1}, i_{A2}) in DF mode with $m_1 = m_2 = 1$ and $f_1 = 50$ Hz, $f_2 = 100$ Hz, (b) output voltages (v_{A1}, v_{A2}) and currents (i_{A1}, i_{A2}) for a sudden change in load under CF mode with same modulation indices $m_1 = m_2 = 1$, (c) DC-link capacitor voltage balancing for a sudden change in load under CF mode with same modulation indices $m_1 = m_2 = 1$	57
3.14	Experimental result in CF mode with $m_1 = m_2 = 1$ (a) output phase voltages ($v_{A1}, v_{A2}, v_{C1}, v_{C2}$), (b) output line voltages (v_{AC1}, v_{AC2}) and currents (i_{A1}, i_{A2}), (c) output currents ($i_{A1}, i_{A2}, i_{C1}, i_{C2}$).	58
3.15	Switching, conduction, and total losses of the proposed TLDO-ANPC for A-phase under CF mode with $m_1 = 1$ and m_2 varying.	61

3.16	Efficiency comparison for (a) CF mode with $m_1 = 1$ (b) CF mode, $m_1 = 0.8$ and $\phi = 30^\circ$, (c) DF mode with $m_1 = 0.5$ and $f_1 = 50$ Hz, $f_2 = 100$ Hz.	62
3.17	Conduction and switching loss comparison at different output powers under CF mode ($m_1 = m_2 = 1$).	62
3.18	Equivalent circuit for the operating states of the proposed TLDO-ANPC (a) $v_{x1} = 0$ and $v_{x2} = -V_{dc}/2$ (b) $v_{x1} = V_{dc}/2$ and $v_{x2} = 0$ (c) $v_{x1} = V_{dc}/2$ and $v_{x2} = -V_{dc}/2$.	63
4.1	(a) Five-level stacked converter for six phase [61]. (b) Three-leg stacked dual-output five-level (TL-SDOFL) converter [73].	66
4.2	Proposed five-level stacked dual output (FLSDO) converter.	67
4.3	Few operating states of the proposed FLSDO (a) $V_{x1} = V_{dc}/2$ and $V_{x2} = 0$ (b) $V_{x1} = +V_{dc}/4$ and $V_{x2} = -V_{dc}/2$ (c) $V_{x1} = -V_{dc}/4$ and $V_{x2} = 0$.	70
4.4	Voltage balancing of DC-link and flying capacitors C_1, C_2, C_{x3} and C_{x4} in the FLSDO converter over a few cycles through the proposed PWM with $m_1 = m_2 = 1, f_1 = f_2 = 50$ Hz.	73
4.5	Normalized capacitor voltage ripple of the FLSDO converter under CF mode with $m_1 = 1$ and $\theta_{L1} = 7.16^\circ$ (a) DC-link capacitor, (b) Flying capacitor.	77
4.6	Boundary region (a) TL-SDOFL (b) FLSDO.	78
4.7	Projections of reference signals onto the FLSDO converter's boundary region under (a) CF with $m_1 = 1, m_2 = 0.9$ and $\phi = 0^\circ$, (b) CF with $m_1 = m_2 = 0.9$ and $\phi = 30^\circ$, (c) DF with $m_1 = m_2 = 1$.	79
4.8	Hybrid PWM scheme for FLSDO (a) CF mode with $m_1 = 1, m_2 = 0.9$ and $\phi = 0^\circ$, (b) CF mode with $m_1 = m_2 = 0.9$ and $\phi = 30^\circ$, (c) DF mode with $m_1 = m_2 = 1, f_1 = 100$ Hz and $f_2 = 50$ Hz.	80
4.9	Developed hardware setup.	83
4.10	Experimental results in CF mode (a) output voltages (v_{A1}, v_{A2}) and currents (i_{A1}, i_{A2}) with $m_1 = m_2 = 0.8$, (b) DC-link and flying capacitor voltage balancing with $m_1 = m_2 = 0.8$, (c) output voltages (v_{A1}, v_{A2}) and currents (i_{A1}, i_{A2}) with $m_1 = 0.8, m_2 = 0.7$, (d) output voltages (v_{A1}, v_{A2}) and currents (i_{A1}, i_{A2}) with $m_1 = m_2 = 0.8$ and $\phi = 30^\circ$.	84
4.11	Experimental results of output voltages (v_{A1}, v_{A2}) and currents (i_{A1}, i_{A2}) (a) in DF mode with $m_1 = m_2 = 0.8$ and $f_1 = 100$ Hz, $f_2 = 50$ Hz, (b) in CF mode with $m_1 = m_2 = 0.8$ for a sudden change in input voltage, (c) in CF mode with $m_1 = m_2 = 0.7$, for a sudden change in load, (d) for a sudden change in m_2 from 0.8 to 1, keeping $m_1 = 0.8$, under CF mode.	85
4.12	Total Harmonic Distortion of output voltages (a) v_{A1} , and (b) v_{A2}	87
4.13	Switching, conduction, and total losses of the proposed FLSDO for phase leg under CF mode with $m_1 = 1$ and m_2 varying.	89
4.14	Efficiency comparison for (a) CF mode with $m_1 = 1$ (b) CF mode, $m_1 = 0.8$ and $\phi = 30^\circ$, (c) DF mode with $m_1 = 0.5$ and $f_1 = 50$ Hz, $f_2 = 100$ Hz.	90
4.15	Five-level stacked multi-output (FLSMO) converter.	91
5.1	Proposed five-level dual output active neutral point clamped (5LDO-ANPC) converter.	94

5.2	Various operating states of the proposed 5LDO-ANPC. (a) $v_{x1} = 0$ and $v_{x2} = V_{dc}/4$. (b) $v_{x1} = V_{dc}/2$ and $v_{x2} = -V_{dc}/4$. (c) $v_{x1} = -V_{dc}/2$ and $v_{x2} = 0$	95
5.3	Graphical depiction of the region of operation and switching states.	102
5.4	Projection of reference signals onto the 5LDO-ANPC converter's boundary region under (a) CF with $m_1 = 1$, $m_2 = 0.9$, (b) CF with $m_1 = m_2 = 0.9$ and phase shift of 30° , (c) CF with $m_1 = m_2 = 0.8$ and phase shift of 60° (d) DF with $m_1 = m_2 = 1$	103
5.5	Block diagram of the FCS-MPC algorithm.	107
5.6	Experimental setup of 5LDO-ANPC.	108
5.7	Simulation result (a) output voltages (v_{A1}, v_{A2}) and currents (i_{A1}, i_{A2}), under CF mode with $m_1 = m_2 = 0.8$, (b) DC-link and flying capacitors voltage balancing under CF mode with $m_1 = m_2 = 0.8$, (c) output voltages (v_{A1}, v_{A2}) and currents (i_{A1}, i_{A2}), under CF mode with $m_1 = m_2 = 0.8$ and phase shift $\phi = 30^\circ$, (d) output voltages (v_{A1}, v_{A2}) and currents (i_{A1}, i_{A2}) under DF mode with $m_1 = m_2 = 0.8$	110
5.8	Simulation result for the output line voltages (v_{ABC1}, v_{ABC2}), currents (i_{ABC1}, i_{ABC2}), speeds (N_1, N_2), and torque (T_1, T_2) for same speed of operation.	111
5.9	Simulation result for the output line voltages (v_{ABC1}, v_{ABC2}), currents (i_{ABC1}, i_{ABC2}), speed (N_1, N_2), and torque (T_1, T_2) for different speed of operation.	111
5.10	Experimental result (a) output voltages (v_{A1}, v_{A2}) and currents (i_{A1}, i_{A2}), $m_1 = m_2 = 0.8$, (b) DC-link and flying capacitors voltage balancing, CF mode $m_1 = m_2 = 0.8$, (c) output voltages (v_{A1}, v_{A2}) and currents (i_{A1}, i_{A2}), $m_1 = 1$, $m_2 = 0.8$, and (d) output voltages (v_{A1}, v_{A2}) and currents (i_{A1}, i_{A2}) having same modulation indices $m_1 = m_2 = 0.8$ and phase shift $\phi = 30^\circ$	112
5.11	Experimental result (a) output voltages (v_{A1}, v_{A2}) and currents (i_{A1}, i_{A2}) with $m_1 = m_2 = 0.8$ under DF mode, (b) sudden change in modulation index of second output terminal under CF mode, (c) output voltages (v_{A1}, v_{A2}) and currents (i_{A1}, i_{A2}) for sudden change frequency of second output terminal with $m_1 = m_2 = 0.8$ and (d) DC-link and flying capacitors voltage balancing for sudden change in modulation index of the second output terminal.	113
5.12	Experimental results under CF mode with modulation indices $m_1 = m_2 = 0.8$: (a) output voltages (v_{A1}, v_{A2}) and corresponding load currents (i_{A1}, i_{A2}) at the start-up, (b) voltage balancing of the DC-link and flying capacitors at the start-up (c) output voltages (v_{A1}, v_{A2}) and corresponding load currents (i_{A1}, i_{A2}) for the shut-down, (d) voltage balancing of the DC-link and flying capacitors for the shut-down.	114
5.13	Total Harmonic Distortion of 5LDO-ANPC at different loads (a) v_{A1} , (b) v_{A2} , (c) i_{A1} , and (d) i_{A2}	117
6.1	TLDO-ANPC fed two motors.	121
6.2	Commutation method and switching states of the TLDO-ANPC converter using IPD-PWM modulation.	122
6.3	Schematic diagram of the field-oriented control for two different motors powered by the TLDO-ANPC converter.	125

6.4	Independent control of two different motors.	126
6.5	Projections of reference signals onto the 5LDO-ANPC converter's boundary region (a) same speed of operation and (b) different speed of operation. . .	127
6.6	Dynamic performance of IM and PMSM under (a) speed variation of the IM and (b) speed variation of the PMSM	129
6.7	DC-link Capacitor voltage balancing.	130
6.8	Test platform.	130
6.9	Experimental Result of line voltages (v_{AB1} , v_{BC1} , v_{AB2} , v_{BC2}), dc-link capacitor voltage (V_{C1} , V_{C2}), direct and quadrature axis currents (i_{d1} , i_{d2} , i_{q1} , i_{q2}) and speed (N_1 , N_2) for IM and PMSM under (a) Same speed of operation, (b) different speed of operation.	131
6.10	Experimental Result of line voltages (v_{AB1} , v_{BC1} , v_{AB2} , v_{BC2}), dc-link capacitor voltage (V_{C1} , V_{C2}), direct and quadrature axis currents (i_{d1} , i_{d2} , i_{q1} , i_{q2}) and speed (N_1 , N_2) for IM and PMSM under (a) speed variation of the IM, and (b) speed variation of the PMSM.	132

List of Tables

2.1	Switching signals and output voltages of the nine-switch inverter.	11
2.2	Switching signals and output voltages of the TPTPMLI.	14
2.3	Switching signal combinations, output voltages, and capacitor currents of the TL-TDI.	15
2.4	Switching signals, output voltages, and capacitor currents of the NPP converter.	17
2.5	Switching signals, output voltages, and capacitor charging state of the DO-FCI	19
2.6	Switching signals, output voltages, and capacitors charging state of the single-phase RSC-DT converter	21
2.7	Switching signals, output voltages, and capacitor currents of the DO-NPC-TLI	24
2.8	Switching signals, output voltages, and capacitor charging state of the NPC-DO	26
2.9	Modified CDOM converter switching states and corresponding output voltage levels and capacitor currents	30
2.10	Graphical representations of different types of operation regions classified by DOC	33
2.11	Graphical representations of different types of operation regions classified by DOC: Back to Back, dual conventional three-level ANPC (CTL-ANPC), and dual flying capacitor ANPC (DFC-ANPC)	36
3.1	Comparison of Single-Phase Dual-Output Three-level Topologies	39
3.2	Switching States, Corresponding Output Voltage and Capacitor Charging State of the TLDO-ANPC	42
3.3	Parameters for Simulation and Hardware	53
4.1	Comparison of the five-level inverter (per leg) for the dual output configuration	68
4.2	FLSDO Switching States, Corresponding Output Voltages and DC-link Capacitor Charging State	71
4.3	Parameters for Experimentation	83
4.4	Comparison of the scalability of the five-level inverter for the different outputs	92
5.1	Comparison of Three-Phase Dual-Output Five-level Topologies	98
5.2	Maximum voltage and current stress on each switch of the 5LDO-ANPC.	99

- 5.3 5LDO-ANPC Switching States, Corresponding Output Voltage, DC-Link and Flying Capacitor Charging State 100
- 5.4 Parameters for Simulation and Hardware 108
- 5.5 Comparison of Current THD 115

- 6.1 Switching States, Corresponding Output Voltage and Capacitor Charging State of the TLDO-ANPC 120
- 6.2 Main Parameters of TLDO-ANPC and Motors. 127

- 7.1 Comparison of TLDO-ANPC, FLSDO, and 5LDO-ANPC Converters 137

Abbreviations

ANPC	Active Neutral Point Clamped
B2B	Back To Back
CHB	Cascaded H-Bridge
CMOM	Cascaded Multi-Output Multilevel
CF	Common Frequency
C5L-ANPC	Conventional Five-level Active Neutral Point
CFLS-MLI	Conventional Five-Level Stacked MLI
DF	Different Frequency
DFC-ANPC	Dual Flying Capacitor Active Neutral Point Clamped
DP	Different Phase
DOC	Dual-Output Converter
EV	Electric Vehicle
ESR	Equivalent Series Resistance
FCS	Finite Control Set
FC	Flying Capacitor
FLSDO	Five-Level Stacked Dual Output

5LDO-ANPC	Five-level Dual-Output Active Neutral Point
IM	Induction Motor
IGBT	Insulated-Gate Bipolar Transistor
IPD-PWM	In-Phase Disposition Pulse-Width Modulation
MOSFET	Metal–Oxide–Semiconductor Field-Effect Transistor
MPC	Model Predictive Control
M-CDOM	Modified Cascaded Dual-Output Multilevel
M-CMOM	Modified Cascaded Multi-Output Multilevel
NPC	Neutral-Point Clamped
NPP	Neutral-Point Piloted
PD-PWM	Phase Disposition Pulse-Width Modulation
PMSM	Permanent Magnet Synchronous Motor
PO	Parallel Output
PV	Photovoltaic
PWM	Pulse-Width Modulation
RES	Renewable Energy Sources
RMS	Root Mean Square
SVM	Space Vector Modulation
TLDO-ANPC	Three-Level Dual-Output Active Neutral-Point Clamped
3PPMLI	Three-Phase Three-Port Multilevel Inverter
TL-SDOFL	Three-Leg Stacked Dual-Output Five-Level
THD	Total Harmonic Distortion

UPS Uninterruptible Power Supply

WTHD Weighted Total Harmonic Distortion

Acknowledgements

While my name appears on the cover of this thesis, its completion is the result of the invaluable support, encouragement, and contributions of many remarkable individuals, to whom I owe my deepest gratitude.

First and foremost, I express my sincere thanks to my supervisor, **Dr. Chinmaya K A**, Department of Electrical Engineering, IIT (BHU) Varanasi. His exceptional mentorship, insightful feedback, and unwavering support have guided me throughout this research journey. His technical expertise and constant motivation have been instrumental in shaping the quality and direction of my work.

I am also deeply grateful to **Dr. Ahmed Hussein** for his helpful suggestions and critical insights that contributed meaningfully to the preparation of manuscript during the course of this research. I extend heartfelt thanks to **Dr. Sandip Ghosh**, Department of Electrical Engineering, IIT (BHU) Varanasi, for his collaborative inputs and valuable guidance, which have significantly enriched the scope and depth of this work.

I would also like to acknowledge the support and cooperation of the technical and administrative staff of the Department of Electrical Engineering, especially **Mr. Dharmendra Kumar Singh**, **Mr. R.C. Sharma**, **Mr. A. N. Singh**, **Mrs. Ranjana Singh**, **Mr. Shirsh Anand**, and **Mr. Anjenya**, for their assistance during the experimental phase of my research.

Besides, I want to express my deepest gratitude to **Dr. Kumar Abhishek Singh**, **Mr. Aditya Kumar** and **Mr. Shiv Prakash**, who supported me throughout my experimental work.

I extend warm thanks to my friends and colleagues **Dr. Ashish Prajapati**, **Mr. Ankit Pratihasta**, **Mr. Anant Kumar**, **Dr. Prateek Utkarsha**, **Mr. Alok Kumar**, **Miss Baby Diana**, **Mrs Rangoli Singh**, **Mrs Saumaya Singh**, **Mr. Prashant Rao** and **Mr. Aakash Ravi** for their constant support, encouragement, and friendship. Their camaraderie and moral support during moments of stress and uncertainty have been deeply appreciated.

I express my deepest gratitude to my parents **late Mr. Sanjeeva Dwivedi** and **Mrs. Anita Dwivedi** whose values, sacrifices, and unwavering belief in me have been my guiding light. Though my father is no longer with us, his presence continues to inspire every milestone of my life.

My heartfelt thanks go to my sister **Miss Vatsala Dwivedi**, for his enduring patience, love, and constant motivation.

Finally, I extend my appreciation to all my extended family members, whose love, good wishes, and emotional strength have helped me remain focused and determined throughout this academic journey. Their support has played a vital role in the successful completion of this thesis.